nature sustainability

Article

https://doi.org/10.1038/s41893-024-01464-x

Chain-length-controllable upcycling of polyolefins to sulfate detergents

Received: 23 May 2024

Accepted: 11 October 2024

Published online: 18 November 2024

Check for updates

Nuwayo Eric Munyaneza[1], Ruiyang Ji[2], Adrian DiMarco[3], Joel Miscall[4,5], Lisa Stanley[4,5], Nicholas Rorrer[4,5], Rui Qiao[2] ✉ & Guoliang Liu[1,3,6] ✉

Escalating global plastic pollution and the depletion of fossil-based resources underscore the urgent need for innovative end-of-life plastic management strategies in the context of a circular economy. Thermolysis is capable of upcycling end-of-life plastics to intermediate molecules suitable for downstream conversion to eventually high-value chemicals, but tuning the molar mass distribution of the products is challenging. Here we report a temperature-gradient thermolysis strategy for the conversion of polyethylene and polypropylene into hydrocarbons with tunable molar mass distributions. The whole thermolysis process is catalyst- and hydrogen-free. The thermolysis of polyethylene and polyethylene/polypropylene mixtures with tailored temperature gradients generated oil with an average chain length of ~C_{14}. The oil featured a high concentration of synthetically useful α-olefins. Computational fluid dynamics simulations revealed that regulating the reactor wall temperature was the key to tuning the hydrocarbon distributions. Subsequent oxidation of the obtained α-olefins by sulfuric acid and neutralization by potassium hydroxide afforded sulfate detergents with excellent foaming behaviour and emulsifying capacity and low critical micelle concentration. Overall, this work provides a viable approach to producing value-added chemicals from end-of-life plastics, improving the circularity of the anthropogenic carbon cycle.

Plastic waste accumulation is a major environmental challenge facing the planet. Globally, 380 megatons of plastics are produced annually, and close to 75% are disposed of after a single use[1]. Polyethylene (PE) and polypropylene (PP), in particular, account for 60% of all plastics and constitute a large proportion of discarded waste[2]. To meaningfully disrupt the plastic waste accumulation trend and minimize carbon emissions, it is critical to increase the recycling rate and extend materials' service life in accordance with the Kyoto Protocols and Paris Accords[3]. Traditional strategies (for example, mechanical recycling) help close the plastic loop, but the quality of the regenerated plastics deteriorates, and market value decreases[4]. After a number of cycles, plastics reach the end of life. Using end-of-life plastics as an inexpensive feedstock for producing value-added chemicals is therefore a highly attractive means to complement traditional approaches[5–7].

In this context, using end-of-life PE and PP as feedstock to produce other high-value chemicals is an enticing strategy[8]. Due to the chemical inertness of backbone C(sp^3)–C(sp^3) bonds in PE and PP, elevated temperatures and long reaction times are required to pyrolyse these polyolefins[9]. For fuel uses, the pyrolysis oil must undergo additional hydrogenation[10] for improved fuel quality. In addition, pyrolysis oil is a complex mixture of hydrocarbons that must be fractionated into naphtha and diesel range hydrocarbons to afford specific transportation fuel grades[11]. A major technical challenge thus remains control over the chain length and its distribution. For lubricant and surfactant applications,

[1]Department of Chemistry, Virginia Tech, Blacksburg, VA, USA. [2]Department of Mechanical Engineering, Virginia Tech, Blacksburg, VA, USA. [3]Department of Chemical Engineering, Virginia Tech, Blacksburg, VA, USA. [4]Renewable Resources and Enabling Sciences Center, National Renewable Energy Laboratory, Golden, CO, USA. [5]BOTTLE Consortium, Golden, CO, USA. [6]Department of Materials Science and Engineering, Macromolecules Innovation Institute, Virginia Tech, Blacksburg, VA, USA. ✉e-mail: ruiqiao@vt.edu; gliu1@vt.edu

https://doi.org/10.1038/s41893-024-01464-x

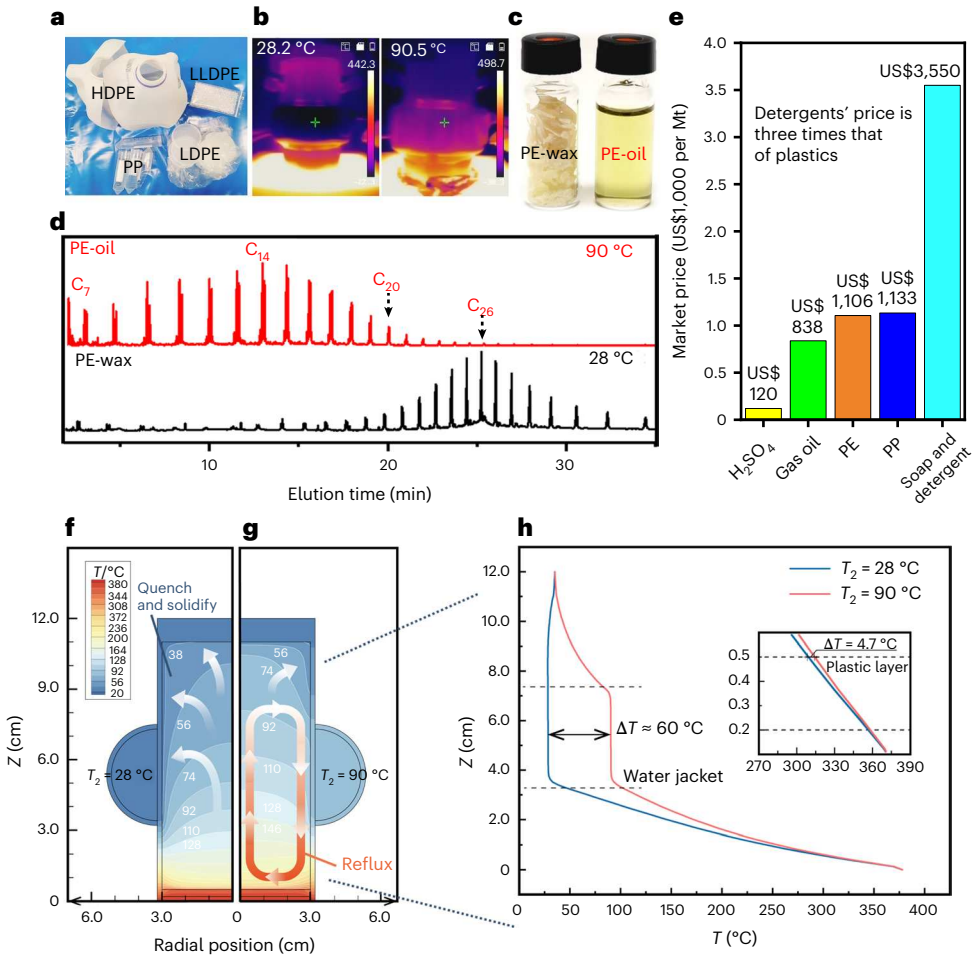

Fig. 1 | Controlling the hydrocarbon product distribution from plastic thermolysis. a, Plastic products used in this work. **b**, Infrared camera photographs showing the temperature of the condensation region. **c**, PE-wax and PE-oil generated upon thermolysis by circulating cold and hot water, respectively. **d**, GC traces of the PE-oil and PE-wax generated from the two sets of conditions. **e**, Market prices of virgin plastics, feedstock chemicals and materials employed, and upcycling products[52–56]. **f**,**g**, Computational fluid dynamics simulated reactor temperature fields: T_2 = 28 °C (left) and T_2 = 90 °C (right). **h**, The temperature profiles along the reactor interior wall. The inset shows the temperature variation in the plastic melt.

the hydrocarbon distribution requirement is even more stringent. Numerous strategies have been tested to control the hydrocarbon distribution, including zeolite-assisted pyrolysis and hydrocracking[12], hydrogenolysis[13], catalytic hydrocracking[14] and cross-alkane metathesis[15] (Supplementary Scheme 1). Generally, these strategies rely on precious-metal catalysts (for example, Ir, Ru and Pt)[16], high H_2 pressures (10–40 bar) and sometimes long reaction times to attain high oil yields, and the hydrocarbon distribution and functionality in the product cannot meet the downstream upcycling needs. Recently, we reported the conversion of PE and PP into intermediate waxes, followed by catalytic oxidation into fatty acids for hard soap[17]. This initial effort proves the concept of the 'plastic-to-soap' strategy, but challenges remain in controlling the hydrocarbon distribution of polyolefin thermolysis products and ensuring a high yield of functional terminal alkenyl groups. For industrial and household detergents and emulsifiers, surfactant molecules with chain lengths of C_{12}–C_{14} are desired, which gives optimal performance[18,19].

Here, by controlling the thermolysis temperature gradient using a simple cooling design, we drastically shift the product hydrocarbon distribution from wax to oil and, importantly, achieve high α-olefin contents. The alkene-rich oil is upcycled into alkyl hydrogensulfates (AHS) through H_2SO_4 treatment followed by neutralization. As an alternative to fuel that has a short life cycle before being released as CO_2 into the atmosphere, AHS retain carbon in a reduced form and are high-value, ubiquitous detergents and emulsifiers in industrial and household applications (Fig. 1e). Typically, AHS are manufactured from oleochemicals and petrochemicals[20]. Using plastic waste as an alternative feedstock reduces the stress on global food resources and fossil fuels[21–24], representing a sustainable means to procure synthetic detergents.

Results

The key to hydrocarbon distribution control is the temperature gradient in our thermolysis process. In our design of temperature-gradient thermolysis, the gradient is controlled by setting the reactor bottom at a high temperature of T_1 and the reactor condenser walls at a lower temperature of T_2. T_1 is sufficiently high to induce polymer chain scission, and T_2 is low enough to quench the chain scission reactions and condense the product. To control the product chain length, we hypothesize that we can simply tune T_2 in the condensation zone. In our previous report[17], cold water circulation in the reactor played a critical role in ensuring that thermolysis did not predominantly produce gaseous products. This observation led us to explore the use of water as a coolant to modulate the temperature gradient and thus the molar mass of the degradation products.

Conversion of PE

To prove the concept, we first subjected high-density PE (HDPE; M_w, 88.38 kDa) to a thermolysis condition of T_1 = 360–400 °C and T_2 = 28 °C

https://doi.org/10.1038/s41893-024-01464-x

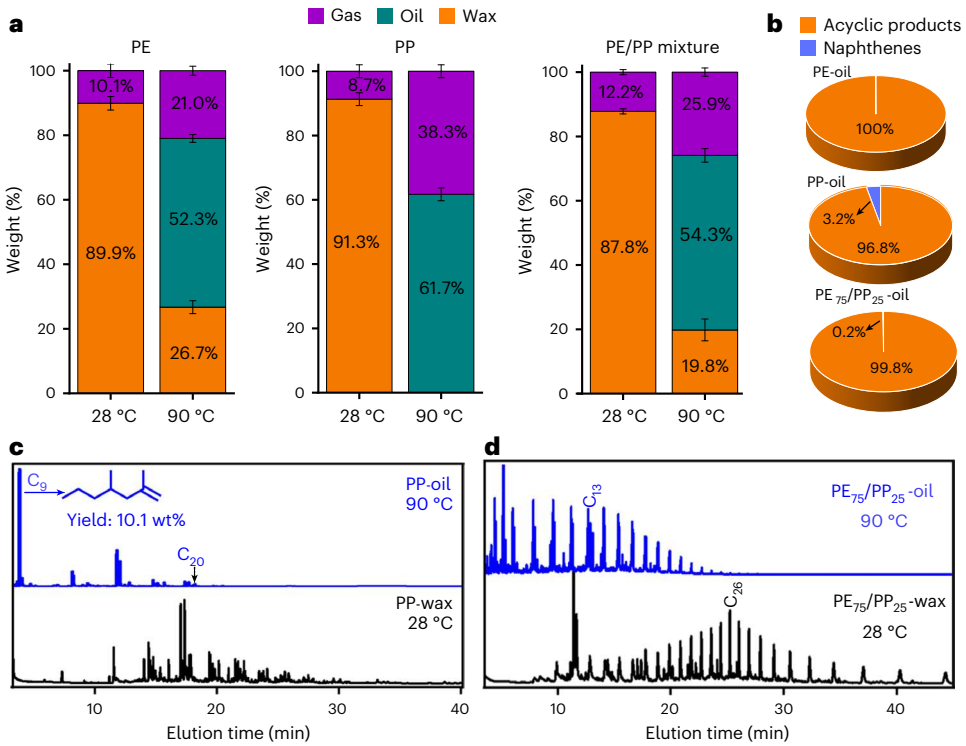

Fig. 2 | Tuning the molar mass of hydrocarbon products from PP and mixed PE_{75}/PP_{25} thermolysis. a, Analysis and quantification of various product phases generated in the thermolysis reaction of PE, PP and a PE/PP mixture (weight ratio of HDPE/LDPE/LLDPE/PP, 25/25/25/25). The values in the bars represent the average yields from three experiments, and the error bars represent their standard deviations. For thermolysis oils, the standard deviation was within ±2.1%. **b**, The weight per cent distribution of naphthenes and acyclic products in PE, PP and PE_{75}/PP_{25} thermolysis oil reveals a high concentration of acyclic alkenes and alkanes. **c**,**d**, GC traces of the oil and wax products from PP and the PE_{75}/PP_{25} mixture under different reaction conditions.

by flowing room-temperature water in the reactor jacket (Fig. 1b, left). This degradation reaction afforded 89.9 wt% wax in the condensation zone consisting of both saturated and unsaturated hydrocarbons (Fig. 2a, left). The gas chromatogram (GC) of the wax in hot hexanes revealed a unimodal distribution centred at C_{26} (Fig. 1d, black curve). In contrast, flowing hot water through the reactor jacket established a T_2 of ~90 °C in the cold trap (Fig. 1b, right). The high T_2 resulted in a different temperature gradient, which furnished ~52.3 wt% oil in the reactor headspace (Fig. 2a, PE at 90 °C; see also Supplementary Fig. 1a). Under the higher-T_2 condition, the components of the oil shifted to lower GC elution times, giving hydrocarbons centred at C_{14} (Fig. 1d, red curve). Further characterization of the thermolysis oil by gas chromatography–mass spectrometry (GC–MS) revealed largely linear alkanes and alkenes along with minor dienes of C_7–C_{20} (Supplementary Fig. 2), with small amounts of hydrocarbons >C_{20}. No cyclic or branched products were detected, suggesting negligible intramolecular and intermolecular radical recombinations under our reaction conditions[25]. In addition to the oil, residual wax (~26.7 wt%) accumulated on the wall after a six-hour reaction. The residual wax revealed alkene and alkane compositions similar to wax collected under T_2 = 28 °C, as confirmed by GC. Besides oil and wax, PE thermolysis produced ~21.0 wt% gaseous products consisting mainly of propane, 2-butene and pentane (Supplementary Fig. 3). Presumably, the 90 °C cold trap liquefied the vaporized hydrocarbons and allowed them to flow back to the reactor bottom, creating a reflux-like phenomenon (Fig. 1g and Supplementary Fig. 4). The observed change in the oil-to-wax selectivity can thus be ascribed to the extensive chain cleavage as a result of 'refluxing' at T_1 = 360–400 °C.

Since it is challenging to precisely measure the temperature field in our reactors, we employed computational fluid dynamics simulations to furnish a detailed picture of this temperature field[26–28]. When T_2 = 28 °C (Fig. 1f), much of the reactor interior wall was at temperatures below the melting points of the wax products, measured to be ~68.8–80.1 °C using a Buchi melting point instrument. As such, driven by diffusion and natural convection (Supplementary Fig. 5), the vaporized wax products were quenched and solidified upon contacting the cold walls. Raising T_2 to 90 °C substantially shrank the region of vertical walls at temperatures below 68.8 °C (Fig. 1g). Hence, vaporized hydrocarbons condensed into liquid on the reactor walls and flew back to the reactor bottom due to gravity (see the arrows in Fig. 1g), as confirmed by our experiments (Supplementary Fig. 4). The hydrocarbon products thus underwent further chain cleavage to produce lighter thermolysis oil. Notably, the temperature in the plastic melt changed by <4.7 °C when T_2 was raised from 28 °C to 90 °C (Fig. 1h, inset). The minor temperature changes in the plastic melt suggest that the tunability of the hydrocarbon chain length is probably not caused by the slight differences in the temperature within the melt layer but originates from the temperature field established in the reactor, especially on the reactor walls. The two reaction conditions demonstrate the potential of controlling the reactor jacket temperature to modulate the chain lengths of thermolysis products.

Further spectroscopic analysis of HDPE-derived hydrocarbons revealed a large amount of α-olefins, which are critical for downstream functionalization. The thermolysis at T_2 = 90 °C demonstrated a higher selectivity towards α-olefins in the oil (90.1 mol% α-olefins and 9.9 mol% internal olefins) than in the wax (78.7 mol% α-olefins and 21.3 mol% internal olefins) (Supplementary Table 1 and Supplementary Fig. 6a). The high selectivity towards terminal alkenes in the oil is probably caused by extensive β-scission, which shortens the product chain length and statistically promotes terminal alkene formation. This conjecture is supported by gel permeation chromatography (GPC) and high-temperature GPC (HT-GPC), which showed a number-averaged

https://doi.org/10.1038/s41893-024-01464-x

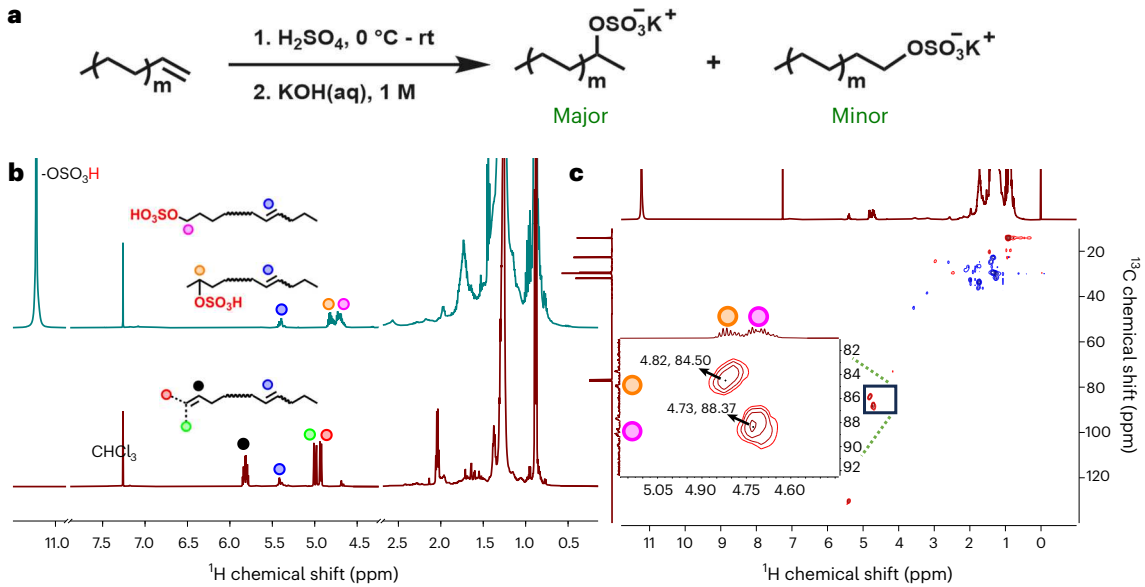

Fig. 3 | Upcycling PE thermolysis oil into sulfate detergents. a, Scheme of the sulfation of alkene oils and subsequent neutralization to ionic detergents. rt, room temperature. **b**, ^{1}H NMR of HDPE oil sulfation in $CDCl_3$. All terminal olefin groups were fully reacted, as evidenced by the disappearance of the green and red proton signals in ^{1}H NMR. **c**, HSQC NMR of HDPE-oil AHS in $CDCl_3$ highlighting the correlation pertaining to the sulfation reaction.

molar mass (M_n) of ~180 g mol^{-1} for the oil versus 380 g mol^{-1} for the wax (Supplementary Table 2 and Supplementary Fig. 7b,c). Notably, the synthetically useful α-olefins in the thermolysis oil consisted of mostly diesel range hydrocarbons (Supplementary Fig. 6c), opening an opportunity for alternative fuel applications.

Conversion of PP and mixed plastics

Similar to HDPE, wax was the main product from PP thermolysis when T_2 = 28 °C (Fig. 2a, middle). When we increased T_2 to 90 °C, thermolysis oil emerged as the main product, giving a yield of 61.7%, similar to previous studies[29] at comparable temperatures (Fig. 2a, middle 'PP at 90 °C'; see also Supplementary Fig. 1b). The thermolysis oil contained predominantly 2,4-dimethyl-1-heptene (~10.1 wt%; Fig. 2c), a common trimer fragment (C_9) from PP degradation[30,31]. Up to 38.3 wt% of PP was converted into gases, probably because PP has easily degradable tertiary C–C bonds. The gas phase was primarily composed of acyclic compounds, including propene, 2-butene and 2-methyl-1-pentene (Supplementary Fig. 8); 1,3,5-trimethylcyclohexane was the only gaseous cycloparaffin detected in the GC–MS. In the end, no wax was collected from the reactor. GC confirmed a narrower product distribution in the oil, mostly ≤C_{20} light hydrocarbons (Fig. 2c). Additionally, GPC and HT-GPC validated the overall decrease in product molar mass upon elevating T_2, showing an M_n of ~565 g mol^{-1} for the wax and ~250 g mol^{-1} for the oil (Supplementary Table 2 and Supplementary Fig. 7b,c). Altogether, these results uphold the practicality of varying temperature gradients in regulating the extent of chain scission in polyolefin thermolysis.

Like PE thermolysis, the alkenyl concentration ($c_{C=C}$) of PP-oil was substantially higher than that of PP-wax (6.75 mmol g^{-1} for PP-oil-90 °C versus 4.61 mmol g^{-1} for PP-wax-28 °C; Supplementary Fig. 9a and Supplementary Table 1). Unlike PE, PP has methyl substitution at every second backbone carbon and offers thermodynamically stable carbon-centred radical intermediates and alkene scission products[32]. Thus, upon thermolysis, PP-oil exhibited higher $c_{C=C}$ than PE-oil. Temperature-gradient heating serves the dual purpose of improving alkenyl group concentration and modulating hydrocarbon distribution. Interestingly, most alkenes in PP-oil were acyclic α-olefins. Internal alkene signals were weak and broad (see ^{1}H nuclear magnetic resonance (NMR) 4.9–5.5 ppm, Supplementary Fig. 9b), but in total, they accounted for ~12.7% of the total alkenyl signals. Furthermore, GC–MS substantiated the predominance of α-olefins, and the most intense peaks corresponded to 2,4-dimethyl-1-heptene, 2,4-dimethyl-1-decene and 4,6,8-trimethyl-1-nonene (Supplementary Fig. 10). Even though PP-oil contained minor cyclic products, including 1,3,5-trimethylcyclohexane (Fig. 2b, middle; and Supplementary Fig. 10, products 3 and 9), acyclic alkenes and alkanes still comprised the majority of PP thermolysis oil.

Considering that real-world plastic waste is a complex mixture, we performed thermolysis of PE with varying amounts of PP. PE/PP mixtures are interesting because these two polyolefins can be easily isolated from other plastics[33] but are hard to separate from each other due to their comparable densities and chemical structures[34]. A PE_{75}/PP_{25} mixture of 25 wt% HDPE (milk jug), 25 wt% low-density PE (LDPE) (container lid), 25 wt% linear low-density PE (LLDPE) (commercial grade) and 25 wt% PP (centrifuge tube) was subject to thermolysis. The PE_{75}/PP_{25} mixture provided a high wax yield of ~87.8 wt% when T_2 = 28 °C and a ~54.3 wt% yield of oil as the major product when T_2 = 90 °C (Fig. 2a, right). The gas phase under T_2 = 90 °C accounted for ~25.9 wt% of the products and comprised light alkenes, including propene, 2-butene and minor ≥C_5 products (Supplementary Fig. 11). As established in single-polymer thermolysis, the hydrocarbon distribution shifted to lower molar masses upon increasing T_2 (Fig. 2d). This observation is further supported by GPC and HT-GPC, which revealed a lower M_n for the oil (~200 g mol^{-1}) than for the wax (~244 g mol^{-1}) from PE_{75}/PP_{25}-mixture thermolysis (Supplementary Table 2 and Supplementary Fig. 7b,c).

The thermolysis of the PE_{75}/PP_{25} mixture yielded products that were characteristic of PE and PP thermolysis. In addition to the typical PE thermolysis linear products, GC–MS revealed PP fragmentation compounds of methyl-substituted acyclic alkane and terminal alkenes (Supplementary Fig. 12). The presence of PP led to the generation of a small amount of cycloparaffins in the oil, such as 1,3,5-trimethylcyclohexane (Supplementary Fig. 12). The mixed-plastic-waste-derived oil exhibited slightly higher selectivity for α-olefins (93.4 mol%) than pure HDPE-oil (Supplementary Table 1). In addition, the mixed-plastic-waste-derived wax under T_2 = 28 °C furnished 84.4 mol% α-olefins (Supplementary Table 1 and ^{1}H-NMR in Supplementary Fig. 13a).

https://doi.org/10.1038/s41893-024-01464-x

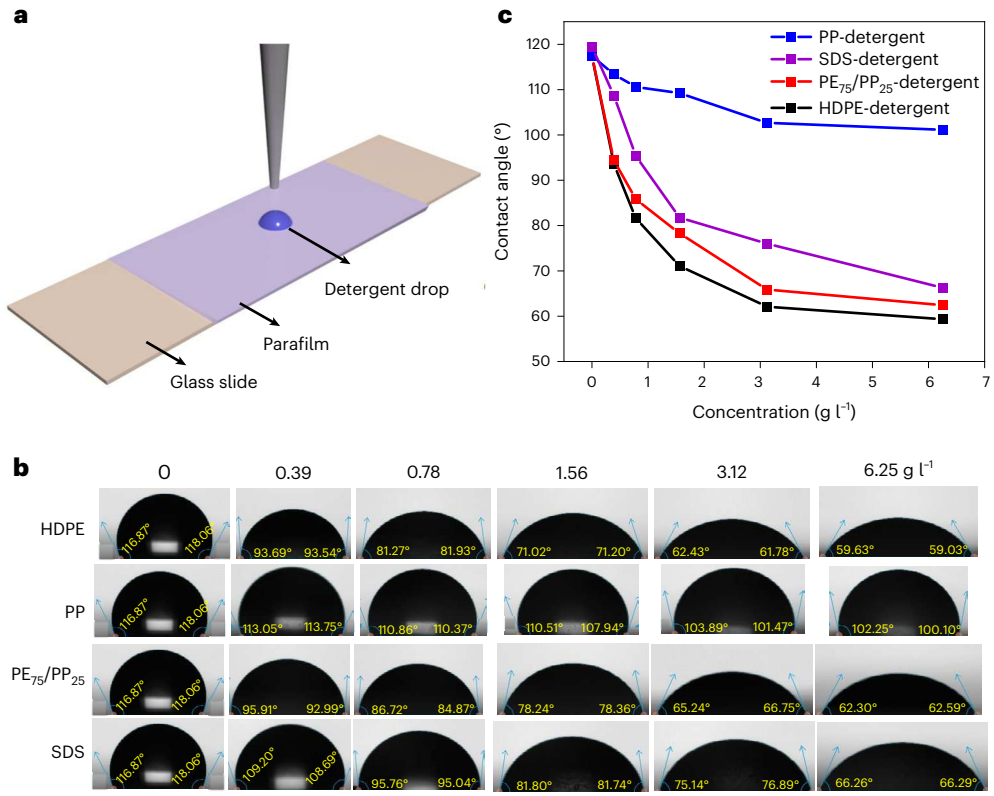

Fig. 4 | Determination of the wettability of PE-, PP-, PE_{75}/PP_{25}- and SDS-detergents. a, Illustration of the substrate for the contact angle measurements. **b**, Photographs of detergent droplets on a glass substrate covered with parafilm. In all cases, the contact angle decreased with increasing detergent concentration. **c**, Contact angle as a function of the PE-, PP-, PE_{75}/PP_{25}- or SDS-detergent concentration.

Upcycling to sulfate detergents

PE-oil and PP-oil can undergo functionalization to produce fatty acids, aldehydes, alcohols and various useful products[35,36]. In this study, we targeted detergents, considering their high demand and market values (Fig. 1e). As a proof of concept, PE and PP thermolysis oils were converted into detergents in two steps. First, chilled oils were reacted with concentrated H_2SO_4 to produce AHS. The hydrogen sulfates were then neutralized with aqueous KOH (1 M) to generate ionic detergents (Fig. 3a). The addition of H_2SO_4 to PE-oil converted all α-alkenyls to AHS, as evidenced by the disappearance of the alkene peaks at 4.90–5.04 ppm and 5.82 ppm in ^{1}H NMR (Fig. 3b). The two new resonance peaks at 4.71 and 4.82 ppm—attributed to the Markovnikov and anti-Markovnikov products, respectively—were correlated to the carbon signals between 84.5 and 88.4 ppm in the 2D ^{1}H-^{13}C heteronuclear single quantum coherence (HSQC) NMR (Fig. 3c). Different from the α-alkenyl groups, the minor internal alkenes were unaffected by the sulfation reaction, probably due to the mild reaction condition. Because alkene groups are present in many surfactant compounds and are beneficial for lathering and moisturizing properties[37], we did not pursue further sulfation of residual internal alkene groups. Similarly, the sulfation reaction effectively transformed PP-oil and PE_{75}/PP_{25}-oil into the corresponding AHS (Supplementary Figs. 14 and 15). The internal alkene groups (6.6 mol% in the mixed oil and 12.7 mol% in PP-oil) were unreacted, as detected in both 1D NMR and HSQC. Eventually, AHS were neutralized and basified with KOH until the pH reached ~9 before further characterization.

Detergent properties were investigated using a theta flow tensiometer and other surfactant analytical techniques. To determine the wettability (a characteristic of how well a surfactant solution spreads across a substrate), we measured the contact angles of a series of detergent concentrations (0 to 6.25 g l^{-1}) on a hydrophobic surface. The hydrophobic surface was created by wrapping a strip of parafilm around a glass slide (Fig. 4a). For all PE-, PP- and PE_{75}/PP_{25}-detergents, the contact angle decreased with increasing detergent concentration (Fig. 4b). PE-detergents showed superior wettability compared with both the mixed and PP counterparts (Fig. 4c). The improved wettability is attributed to the favourable interactions between the detergents' alkyl chains and the hydrophobic parafilm chains at the interface. Conversely, the incorporation of methyl-substituted chains in PP-oil, mostly short-chain 2,4-dimethyl-1-heptene, hindered the same interchain interactions, probably because of the poor chain flexibility[38]. The introduction of PP-derived molecules in the mixed detergent formulations therefore slightly worsened the wettability (Fig. 4b, red curve). Nevertheless, adequate wettability was maintained at PP loadings of up to 10 wt% (Supplementary Fig. 16). For comparison, commonly used sodium dodecyl sulfate (SDS) exhibited greater wettability than PP-derived detergent (Fig. 4c). However, PE and PE_{75}/PP_{25}-derived detergents outperformed SDS in terms of wettability. High PP loading in the feedstocks (>25%) results in detergents of poor wettability, probably because of the extensive substitution of the alkyl chains.

PE- and PE_{75}/PP_{25}-derived ionic detergents displayed excellent foaming behaviour and emulsifying capacity at room temperature. PE-detergent exhibited a well-sustained foamy lather over one hour (Fig. 5a, first row). In contrast, PP- and PE_{75}/PP_{25}-detergents could not sustain a stable foamy lather (Fig. 5a, second and third rows), presumably because of the defoaming characteristic of branched chains[39]. Nonetheless, the low-foam feature of PP-detergent can be exploited to formulate PE/PP mixed surfactants presenting excellent wettability and defoaming performance for industrial applications[40]. Furthermore, an effective detergent should have an affinity for both water and organic substances to achieve amphiphilicity. To determine the emulsifying power of the plastic-waste-derived detergents, we recorded the time for

https://doi.org/10.1038/s41893-024-01464-x

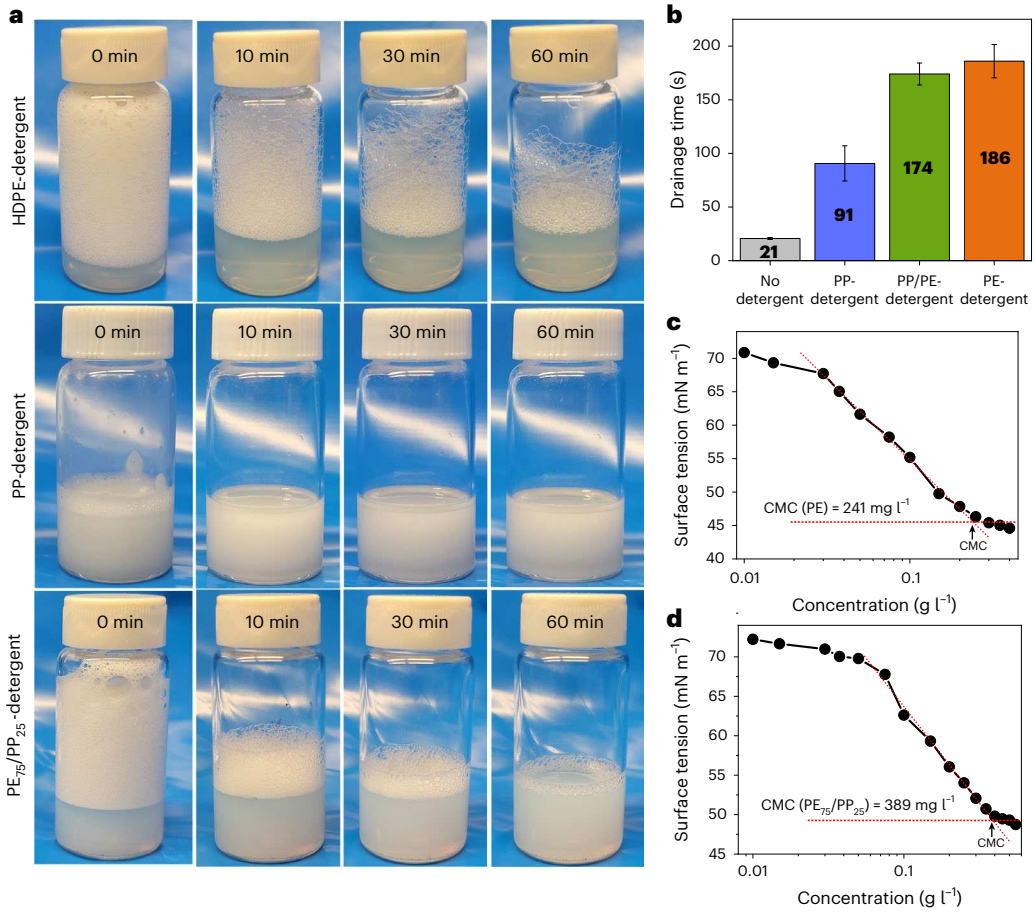

Fig. 5 | Physicochemical properties of sulfate detergents. a, Foam stability of HDPE-, PP- and PE_{75}/PP_{25}-derived detergents. HDPE-detergent exhibited higher foam stability than PP- or PE_{75}/PP_{25}-detergent. **b**, The emulsifying power of detergents was obtained by recording the separation time of 10 ml of water from a mixture of paraffin oil and water. The values in the bars represent the average drainage time of three experiments, and the error bars represent their standard deviations. **c**,**d**, Surface tension as a function of PE-detergent concentration (**c**) and PE_{75}/PP_{25}-detergent concentration (**d**) to determine CMC.

10 ml of water to separate from a mixture of paraffin oil and water (foam drainage process; Supplementary Fig. 17)[41]. In the absence of a detergent, the separation was swift, and 21 s was sufficient to isolate 10 ml of water from the mixture (Fig. 5b). The addition of PP- or PE-detergent at a concentration of 1.25 mg ml^{-1} drastically bolstered the drainage time to 91 s or 186 s, respectively. Remarkably, PE_{75}/PP_{25}-detergent also demonstrated great emulsification performance comparable to that of pure PE-detergent, illustrating the feasibility of turning unsorted mixed polyolefin wastes into sustainable emulsifiers. Besides paraffin oil, the detergent solutions (1.2 ml) mixed well with 50 µl of hexanes, which further corroborates their excellent emulsification properties (Supplementary Fig. 18).

To study the detergents' ability to lower water surface tension (γ), we prepared a series of detergent solutions with varying concentrations and examined γ using a theta flow tensiometer in a pendant-drop mode. PE-detergent displayed a critical micelle concentration (CMC) of 241 mg l^{-1} and exhibited the highest reduction in γ at the air–water interface (γ_{CMC} = 45.5 mN m^{-1}; Fig. 5c). PP-detergent produced small changes in γ at low concentrations and only underwent micellization at higher concentrations (γ_{CMC} = 51.6 mN m^{-1}, CMC = 518 mg l^{-1}; Supplementary Fig. 19a), as a consequence of poor hydrophobicity and aggregation of short alkyl chains[42]. Accordingly, the inclusion of 25 wt% PP in the PE_{75}/PP_{25} mixture precursor led to a CMC value of 389 mg l^{-1} and γ_{CMC} of 49.3 mN m^{-1} for PE_{75}/PP_{25}-detergent (Fig. 5d). Nonetheless, detergents derived from mixed PE/PP waste containing up to 10 wt% PP still exhibited a high reduction in γ (γ_{CMC} = 48.4 mN m^{-1}) at a relatively low CMC of 238 mg l^{-1}, on par with pure PE-detergent (Supplementary Fig. 19b), which suggests the latter's ability to tolerate 'polymer contaminations'. Compared with some benchmark detergents, such as SDS (CMC > 2 g l^{-1})[43], the CMC of PE- and PE/PP-mixture-derived detergents is lower, illustrating their excellent performance even at low concentrations.

Discussion

Over the past few decades, single-use plastics have continued to accumulate in the environment, and concerted efforts have been made to curb this pollution crisis. Using plastic waste as feedstocks to synthesize useful chemicals is among the most promising approaches. Our method herein employs underutilized plastic waste as a resource to generate high-value detergents. Modulating the temperature gradient in our custom-designed thermolysis reactor effectively adjusted the molar mass of hydrocarbons, enabling the production of thermolysis oils instead of waxes. We further valorized the hydrocarbon intermediates to furnish ionic detergents by reacting the olefins with H_2SO_4. All detergents displayed superior emulsifying power and substantially reduced the surface tension of the air–water interface at low detergent concentrations.

Compared with conventional hydrocracking strategies, our hydrogen-free thermolysis process produces substantial amounts of olefinic hydrocarbons that can be chemically transformed into high-value products[44,45]. The relatively mild thermolysis conditions are key to minimizing the generation of low-value char and coke, typically seen for reactions at temperatures above 450 °C[46]. To further improve the carbon efficiency and overall sustainability, it is essential to boost

the alkene-to-alkane ratio in the thermolysis products. Nonetheless, the saturated alkanes can be valorized into functional chemicals via oxidation using inorganic catalysts or microorganisms[47,48]. Alternatively, the alkanes can be used directly as diesel fuel without additional hydrogenation[49]. It is noteworthy that naphthenes observed in the PP-oil are allowed in diesel formulations, and they can make up >30% of the total composition[50]. Future studies should also explore the possibility of upcycling into terminal AHS exclusively, which can be achieved through converting α-olefins into terminal fatty alcohols via hydroboration, followed by oxidation with air/SO_3. Terminal AHS may perform better than secondary AHS; however, the trade-off is that the synthesis involves more steps, thus potentially adding costs to large-scale production.

This work highlights a viable chemical upcycling strategy to obtain high-value products from plastic waste while contributing to the goal of achieving a circular economy. The presented methodology can potentially reduce the consumption of petrochemicals in detergent manufacturing. Compared with using plant-based oleochemicals (for example, agricultural fatty acids), the current process does not compete with food resources for raw materials or take up any agricultural land. A plastic-waste-based detergent industry does not exacerbate deforestation as do oleochemicals, and therefore presents a sustainable approach to accessing detergents. The use of cooling fluids to modulate the temperature gradient and control thermolysis product distributions demonstrates the versatility, effectiveness and practicality of our temperature-gradient thermolysis to procure detergent precursors from low-cost plastic waste resources.

Methods

Materials

Deuterated benzene (C_6D_6, 99.8%; Cambridge Isotope Laboratories), deuterated chloroform ($CDCl_3$, 99.8%; Cambridge Isotope Laboratories), sulfuric acid (98.0%; Fisher Scientific), hexanes (≥98.5%; VWR Chemicals), 1-dodecene (95%; Sigma-Aldrich), isopentane (≥99.5%; Sigma-Aldrich), *n*-decane (99%; Fisher Scientific), potassium hydroxide (pure pellets; Sigma-Aldrich), sodium hydroxide (pure pellets; Sigma-Aldrich), borane tetrahydrofuran complex solution (1.0 M in tetrahydrofuran (THF); Sigma-Aldrich) and hydrogen peroxide (30 wt%; Fisher Scientific) were purchased and used as received. HDPE (milk jug), LDPE (container lid) and PP (centrifuge tube) were obtained locally in Blacksburg, Virginia, followed by washing and air drying before pulverization. LLDPE pellets (commercial grade) were used without further purification. All polymers were pulverized into powders in a Homend pulverizer for 15 min (5 min, three times) before thermolysis.

Instrumentation

GC and flame ionization detector. Most GC analyses were carried out on a Hewlett Packard HP 5890 Series II Gas Chromatograph equipped with a DB-5 capillary column (30 m × 0.25 mm × 0.25 µm) and a flame ionization detector. The following conditions were applied: helium column flow rate, 11 ml min^{-1}; injection port temperature, 280 °C; detector temperature, 280 °C; initial column temperature, 50 °C; ramp rate, 10 °C min^{-1}; final column temperature, 280 °C. The GC analyses in Supplementary Figs. 20–23 and 28–30 were carried out on an Agilent 7890A Gas Chromatograph System equipped with an HP-5 capillary column (30 m × 0.32 mm × 0.25 µm) and a flame ionization detector. The following conditions were applied: carrier gas column flow rate, 11 ml min^{-1}; injection port temperature, 280 °C; detector temperature, 280 °C; initial column temperature, 40 °C; ramp rate, 10 °C min^{-1}; final column temperature, 280 °C. For sample preparation, typically, 10–15 mg of oil or wax was dissolved in 10 ml of hexanes or toluene. The oil solutions were stirred at room temperature until complete dissolution, and the waxes were stirred at 70 °C until all solids were dissolved. The samples were filtered through a 0.45 µm PTFE filter, and 1 µl of each sample was injected into the GC. Triacontane was used as an internal standard for all weight fraction evaluations.

GC–MS. All GC–MS analyses were performed using a 6890 coupled with a 5973 MSD from Agilent. Separations were obtained using a DB-5 column (30 m, 250 µm inner diameter (ID), with a film thickness of 0.25 µm). The following operating conditions were used for the analyses:

Injection port temperature	280 °C
Split valve	1/25
Purge flow	3 ml min^{-1}
Constant flow	1 ml min^{-1}
Injection volume	1 µl
Column oven initial temperature	50 °C
Column initial time	3 min
Column oven ramp rate	10 °C min^{-1}
Column oven final time	280 °C
MS transfer line temperature	250 °C
MS database	Wiley
MS scan mod range	10–800

HT-GPC. HT-GPC of PE- and PP-derived waxes was performed using a Tosoh EcoSec HLC-8321 High-Temperature GPC System with an autosampler and a differential refractive index detector. The temperature settings were as follows: solvent stocker at 40 °C, pump oven at 50 °C, column oven at 160 °C, refractive index detector at 160 °C, injector valve at 160 °C and autosampler at 160 °C. The mobile phase was 1,2,4-trichlorobenzene (TCB) (Sigma Aldrich-HPLC Grade-256412). The TCB solvent was used as received, and no inhibitor was added. The sample columns were set to an operating flow rate of 1.0 ml min^{-1}, and the reference column was set to an operating flow rate of 0.5 ml min^{-1}. A 300 µl sample loop was used for sample injection. Polymer separation was performed using four Tosoh TSKgel columns attached in the following order: one TSKgel guard column HHR (30) HT2 7.5 mm ID × 7.5 cm (PN 22891), two TSKgel G2000 HHR (20) HT2 7.8 mm ID × 30 cm columns (PN 22890) and one TSKgel GMH HR-H (S) HT2 7.8 mm ID × 30 cm column (PN 22889). Tosoh 10 ml high-temperature sample vials with PTFE caps were used for sample preparation. 6–16 mg of sample was added to a 10 ml sample vial, and TCB solvent was then added to reach an end concentration of ~1.6 mg ml^{-1}. PE- and PP-derived waxes were heated at 160 °C for 1 h directly on the autosampler. The samples were not filtered. Tosoh's Polystyrene-Quick Kit-M (PN 21916) was used to create the calibration curve. The calibration curve was verified using Tosoh polystyrene F-10 (106 kDa—PN 05210)) and Agilent polystyrene (700 Da—PN PSS-ps700) standards. The run time for all standards and samples was 60 min. For data analysis, Eco-Sec 8321 software (Tosoh) was used to evaluate the calibration curves and determine the molar mass and dispersity values. All polymer refractive index peaks were integrated from the point where they first deviated from the baseline to where the refractive index signal returned to the baseline again. Mark–Houwink correction values were used to determine PE and PP molar mass. The Mark–Houwink values used for polystyrene were $K = 12.1 \times 10^{-5}$ dl g^{-1} and $\alpha = 0.707$. The Mark–Houwink values used for PE were $K = 40.6 \times 10^{-5}$ dl g^{-1} and $\alpha = 0.725$. The Mark–Houwink values used for PP were $K = 19.0 \times 10^{-5}$ dl g^{-1} and $\alpha = 0.725$.

Ambient-temperature GPC. To prevent the evaporation of oils at high temperatures, room-temperature GPC was used to characterize the molar masses of thermolysis oils. 15–20 mg of sample was dissolved in THF to achieve a concentration of ~2 mg ml^{-1} and stirred for 30 min. The THF solution was filtered through a 0.2 µm syringe filter into an HPLC

vial. 20 µl of sample was injected into an HPLC fitted with three PLgel 7.5 mm × 300 mm columns in the series 10 µm × 50 Å, 10 µm × 103 Å and 10 µm × 104 Å (Agilent Technologies) at ambient temperature with an isocratic 1 ml min^{-1} 100% THF (Sigma-Aldrich inhibitor-free, suitable for HPLC ≥ 99.9%) for 40 min. Analytes are monitored at 210 nm, 260 nm and 270 nm on the diode-array detection.

NMR. All ^{1}H NMR experiments were performed at 298 K on a 500 MHz Bruker Avance II 500 spectrometer with 16 scans. All spectra were recorded using deuterated benzene and chloroform. ^{13}C NMR experiments for oils were conducted at 298 K on a 500 MHz Bruker Avance II 500 spectrometer using a relaxation delay of 2 s and 1,024 scans. ^{13}C NMR experiments for AHS were performed using a relaxation delay of 6 s and 3,072 scans. 2D-HSQC was conducted at 298 K on a 500 MHz Bruker Avance III 500 spectrometer with a relaxation time of 2 s, 16 scans and a digitizing increment of 400.

Theta flow tensiometer. Contact angle and surface tension were measured at room temperature on a Biolin Scientific theta flow tensiometer. Contact angle experiments were performed in a sessile drop mode with a drop volume of ~5 µl, a drop rate of 1 µl s^{-1} and a run time of ~10 s. Surface tensions were evaluated in a pendant drop mode with a drop volume of ~10 µl, a drop rate of 1 µl s^{-1} and a run time of ~10 s.

Thermolysis procedures

Typically, 1.5 g of pulverized HDPE (particle size, 2.7 mm) or PP (particle size, 1.6 mm) was loaded into a custom-designed quartz reactor and purged with nitrogen at 200 °C for 15 min. After purging, the temperature was slowly ramped (rate, 20 °C min^{-1}) to the operational temperature range (the top layer of the plastic melt was ~360 °C). At the same time, room-temperature water or heated water was circulated in the reactor jacket. After 10 min, the cold-zone temperature stabilized at ~28 °C or ~90 °C. The thermolysis lasted for 6 h for HDPE and 2 h for PP. After completion, the thermolysis oil in the headspace was collected using a glass pipette and weighed on an analytical balance. Solid wax was extracted from the reactor with hexanes twice (10 ml each), dried under vacuum and weighed to determine the yield.

To upcycle PE- and PP-oil to sulfate detergents, 100 mg of each oil was weighed and transferred to a flame-dried 25 ml vial fitted with a stir bar. The test tube was set in a cold bath at 0 °C, and 50 mg of concentrated sulfuric acid was added dropwise while stirring. For PP-oil, 86.7 mg of H_2SO_4 was used. After 10 min, the vial and its contents were stirred at room temperature for 10 min and then neutralized with 1 M KOH solution (1.2 ml) to afford the ionic detergents. The detergent solutions were diluted with DI water to a total volume of 8 ml. The unconverted alkane component was isolated by washing the crude solution with hexanes (5 ml, 3×). The combined hexane extracts were dried over Na_2SO_4, concentrated under vacuum and weighed. An aliquot of the sample was subject to GC and GC–MS characterization. To remove any residual hexanes in the purified detergent solution, a moderate vacuum of 300 mmHg was applied to the detergent vial at 45 °C for 10 min.

Alternatively, selective upcycling of the thermolysis oils to terminal fatty alcohols was accomplished through hydroboration. Typically, 500 mg of PE-oil (~1.9 mmol of alkene, 1 eq.) was added to a two-neck round-bottom flask equipped with a stir bar. The flask was purged with nitrogen and transferred to an ice-water bath. Then, 4.0 ml (~4.0 mmol, 2.1 eq.) of borane tetrahydrofuran complex solution (BH_3·THF, 1.0 M in THF) was dispensed into the flask over a 30-minute period. The flask was warmed to room temperature and stirred for 2 h. Excess BH_3·THF was decomposed by adding 1 ml of DI water until bubbling stopped. The flask was placed back into an ice-water bath. Then, 5.4 ml of 3 M NaOH and 5.4 ml of H_2O_2 (30 wt%) were added dropwise sequentially. The flask was allowed to warm to room temperature and stirred overnight. After completion, the solution was worked up in a separatory funnel using ether and DI water (30 ml each). The water layer was extracted with additional ether (10 ml, 2×) to recover any residual fatty alcohols. The combined organic layer was washed with DI water (50 ml, 3×). The ether extracts were dried over Na_2SO_4, concentrated under vacuum and characterized with NMR and Fourier transform infrared spectroscopy. PP- and PE_{75}/PP_{25}-derived fatty alcohols were prepared similarly.

Simulations

Computational fluid dynamics (CFD) simulations were conducted to analyze the fluid flow and heat transfer within the reactor. The meshing was carried out using ANSYS ICEM CFD 2023 R2, and the simulations were performed using ANSYS FLUENT 2023 R2. Detailed descriptions of the physical models, numerical setup, and simulation parameters can be found in the supplementary information.

Reporting summary

Further information on research design is available in the Nature Portfolio Reporting Summary linked to this article.

Data availability

Additional data are provided in the Supplementary Information, and all the raw files are available via Dryad at https://doi.org/10.5061/dryad.41ns1rnq0 (ref. 51). Source data are provided with this paper.

References

1. Celik, G. et al. Upcycling single-use polyethylene into high-quality liquid products. *ACS Cent. Sci.* **5**, 1795–1803 (2019).
2. Butler, E., Devlin, G. & McDonnell, K. Waste polyolefins to liquid fuels via pyrolysis: review of commercial state-of-the-art and recent laboratory research. *Waste Biomass Valor.* **2**, 227–255 (2011).
3. Schleussner, C.-F., Ganti, G., Rogelj, J. & Gidden, M. J. An emission pathway classification reflecting the Paris Agreement climate objectives. *Commun. Earth Environ.* **3**, 135 (2022).
4. Ellis, L. D. et al. Chemical and biological catalysis for plastics recycling and upcycling. *Nat. Catal.* **4**, 539–556 (2021).
5. Zhang, F. et al. Polyethylene upcycling to long-chain alkylaromatics by tandem hydrogenolysis/aromatization. *Science* **370**, 437–441 (2020).
6. Liu, S., Kots, P. A., Vance, B. C., Danielson, A. & Vlachos, D. G. Plastic waste to fuels by hydrocracking at mild conditions. *Sci. Adv.* **7**, eabf8283 (2021).
7. Dong, Q. et al. Depolymerization of plastics by means of electrified spatiotemporal heating. *Nature* **616**, 488–494 (2023).
8. Thiounn, T. & Smith, R. C. Advances and approaches for chemical recycling of plastic waste. *J. Polym. Sci.* **58**, 1347–1364 (2020).
9. Lv, H., Huang, F. & Zhang, F. Upcycling waste plastics with a C–C backbone by heterogeneous catalysis. *Langmuir* **40**, 5077–5089 (2024).
10. Bezergianni, S., Dimitriadis, A., Faussone, G.-C. & Karonis, D. Alternative diesel from waste plastics. *Energies* **10**, 1750 (2017).
11. Dobó, Z. et al. Characterization of gasoline-like transportation fuels obtained by distillation of pyrolysis oils from plastic waste mixtures. *Energy Fuels* **35**, 2347–2356 (2021).
12. Kots, P. A., Doika, P. A., Vance, B. C., Najmi, S. & Vlachos, D. G. Tuning high-density polyethylene hydrocracking through mordenite zeolite crystal engineering. *ACS Sustain. Chem. Eng.* **11**, 9000–9009 (2023).
13. Tennakoon, A. et al. Catalytic upcycling of high-density polyethylene via a processive mechanism. *Nat. Catal.* **3**, 893–901 (2020).
14. Vance, B. C. et al. Single pot catalyst strategy to branched products via adhesive isomerization and hydrocracking of polyethylene over platinum tungstated zirconia. *Appl. Catal. B* **299**, 120483 (2021).

15. Jia, X., Qin, C., Friedberger, T., Guan, Z. & Huang, Z. Efficient and selective degradation of polyethylenes into liquid fuels and waxes under mild conditions. *Sci. Adv.* **2**, e1501591 (2016).
16. Gan, L. et al. Beyond conventional degradation: catalytic solutions for polyolefin upcycling. *CCS Chem.* **6**, 313–333 (2023).
17. Xu, Z. et al. Chemical upcycling of polyethylene, polypropylene, and mixtures to high-value surfactants. *Science* **381**, 666–671 (2023).
18. Cox, M. F. Effect of alkyl carbon chain length and ethylene oxide content on the performance of linear alcohol ether sulfates. *J. Am. Oil Chem. Soc.* **66**, 1637–1646 (1989).
19. *Soaps & Detergents* (Eastman, 2024); https://www.eastman.com/Markets/cleaners/Household-Cleaners/Pages/Soaps-Detergents.aspx
20. Chupa, J., Misner, S., Sachdev, A., Wisniewski, P. & Smith, G. A. in *Handbook of Industrial Chemistry and Biotechnology* (ed. Kent, J. A.) 1431–1471 (Springer US, 2012).
21. Thannimalay, L. & Yusoff, S. Comparative analysis of environmental evaluation of LAS and MES in detergent—a Malaysian case study. *World Appl. Sci. J.* **31**, 1635–1647 (2014).
22. Lucchetti, M. G., Paolotti, L., Rocchi, L. & Boggia, A. The role of environmental evaluation within circular economy: an application of life cycle assessment (LCA) method in the detergents sector. *Environ. Clim. Technol.* **23**, 238–257 (2019).
23. Liu, B. et al. Corncob cellulose nanosphere as an eco-friendly detergent. *Nat. Sustain.* **3**, 448–458 (2020).
24. Farias, C. B. B. et al. Production of green surfactants: market prospects. *Electron. J. Biotechnol.* **51**, 28–39 (2021).
25. Aguado, J., Serrano, D. & Escola, J. in *Feedstock Recycling and Pyrolysis of Waste Plastics: Converting Waste Plastics into Diesel and Other Fuels—Catalytic Upgrading of Plastic Wastes* (eds John Scheirs, J. & Kaminsky, W.) Ch. 3, 73–110 (Wiley, 2006).
26. Mazloum, S. et al. Modelling plastic heating and melting in a semi-batch pyrolysis reactor. *Appl. Energy* **283**, 116375 (2021).
27. De la Flor-Barriga, L. A. & Rodríguez-Zúñiga, U. F. Numerical analysis on a catalytic pyrolysis reactor design for plastic waste upcycling using CFD modelling. *RSC Adv.* **12**, 12436–12445 (2022).
28. Shan, T. et al. Simulation of the two-stage pyrolysis process of mixed waste plastics. *Energy Fuels* **37**, 16771–16780 (2023).
29. Ahmad, I. et al. Pyrolysis study of polypropylene and polyethylene into premium oil products. *Int. J. Green. Energy* **12**, 663–671 (2015).
30. De Amorim, M. T. S. P., Comel, C. & Vermande, P. Pyrolysis of polypropylene: I. Identification of compounds and degradation reactions. *J. Anal. Appl. Pyrolysis* **4**, 73–81 (1982).
31. Ballice, L. & Reimert, R. Classification of volatile products from the temperature-programmed pyrolysis of polypropylene (PP), atactic-polypropylene (APP) and thermogravimetrically derived kinetics of pyrolysis. *Chem. Eng. Process. Process Intensif.* **41**, 289–296 (2002).
32. Das, P. & Tiwari, P. Valorization of packaging plastic waste by slow pyrolysis. *Resour. Conserv. Recycl.* **128**, 69–77 (2018).
33. Serranti, S., Luciani, V., Bonifazi, G., Hu, B. & Rem, P. C. An innovative recycling process to obtain pure polyethylene and polypropylene from household waste. *Waste Manage. (Oxf.)* **35**, 12–20 (2015).
34. Bauer, M. et al. Sink–float density separation of post-consumer plastics for feedstock recycling. *J. Mater. Cycles Waste Manage.* **20**, 1781–1791 (2018).
35. Kanbur, U. et al. Catalytic carbon–carbon bond cleavage and carbon-element bond formation give new life for polyolefins as biodegradable surfactants. *Chem* **7**, 1347–1362 (2021).
36. Li, H. et al. Hydroformylation of pyrolysis oils to aldehydes and alcohols from polyolefin waste. *Science* **381**, 660–666 (2023).
37. Prieto Vidal, N. et al. The effects of cold saponification on the unsaponified fatty acid composition and sensory perception of commercial natural herbal soaps. *Molecules* **23**, 2356 (2018).
38. Wilkinson, K. M., Bain, C. D., Matsubara, H. & Aratono, M. Wetting of surfactant solutions by alkanes. *ChemPhysChem* **6**, 547–555 (2005).
39. Yang, L., Li, X. & Dong, J. Renewable branched-chain sulfonate surfactants by addition of sodium hydrogensulfite to alkyl oleate. *Colloids Surf. A* **641**, 128513 (2022).
40. Ju, Y., Hua, J., Niu, H. & Chen, H. Multibranched molecule defoamers based on methyl gallate for highly effective defoaming and antifoaming. *Langmuir* **39**, 12497–12509 (2023).
41. Li, J., Li, Y., Song, Y., Wang, Z. & Zhang, Q. Properties of quaternary ammonium surfactant with hydroxyethyl group and anionic surfactant mixed systems. *J. Mol. Liq.* **271**, 373–379 (2018).
42. Bijma, K. et al. Classification of calorimetric titration plots for alkyltrimethylammonium and alkylpyridinium cationic surfactants in aqueous solutions. *J. Chem. Soc. Faraday Trans.* **93**, 1579–1584 (1997).
43. Markarian, S. A., Harutyunyan, L. R. & Harutyunyan, R. S. The properties of mixtures of sodium dodecylsulfate and diethylsulfoxide in water. *J. Solut. Chem.* **34**, 361–368 (2005).
44. Bäckström, E., Odelius, K. & Hakkarainen, M. Trash to treasure: microwave-assisted conversion of polyethylene to functional chemicals. *Ind. Eng. Chem. Res.* **56**, 14814–14821 (2017).
45. Chen, L. et al. Selective, catalytic oxidations of C–H bonds in polyethylenes produce functional materials with enhanced adhesion. *Chem* **7**, 137–145 (2021).
46. Onwudili, J. A., Insura, N. & Williams, P. T. Composition of products from the pyrolysis of polyethylene and polystyrene in a closed batch reactor: effects of temperature and residence time. *J. Anal. Appl. Pyrolysis* **86**, 293–303 (2009).
47. Albonetti, S., Cavani, F. & TrifirÒ, F. Key aspects of catalyst design for the selective oxidation of paraffins. *Catal. Rev.* **38**, 413–438 (1996).
48. Raymond, R. L. Microbial oxidation of *n*-paraffinic hydrocarbons (volume 2). *J. Ind. Microbiol. Biotechnol.* **22**, 206–215 (1999).
49. Ardiyanti, A. R., Khromova, S. A., Venderbosch, R. H., Yakovlev, V. A. & Heeres, H. J. Catalytic hydrotreatment of fast-pyrolysis oil using non-sulfided bimetallic Ni–Cu catalysts on a δ-Al2O3 support. *Appl. Catal. B* **117–118**, 105–117 (2012).
50. Clothier, P. Q. E., Aguda, B. D., Moise, A. & Pritchard, H. O. How do diesel-fuel ignition improvers work? *Chem. Soc. Rev.* **22**, 101–108 (1993).
51. Munyaneza, N. E. et al. Chain-length-controllable upcycling of polyolefins to sulfate detergents. *Dryad* https://doi.org/10.5061/dryad.c866t1gc5 (2024).
52. *U.S. Soap and Detergent Market: Analysis and Forecast to 2030* (IndexBox, 2022).
53. *Price of High-Density Polyethylene Worldwide from 2017 to 2022* (Statista, 2023).
54. *Price of Polypropylene Worldwide from 2017 to 2022* (Statista, 2023).
55. *U.S.—Sulphuric Acid and Oleum—Market Analysis, Forecast, Size, Trends and Insights* (IndexBox 2023).
56. *Markets/Energy-Refined Products* (Bloomberg, 2024); https://www.bloomberg.com/energy

Acknowledgements

This work is based on the project supported by NSF Award No. DMR-2411680. We acknowledge the Chemistry Chromatography Center at Virginia Tech and M. Ashraf-Khorassani for providing assistance with the GC–MS experiments.

Author contributions

G.L. conceived and supervised the project. G.L. and N.E.M. designed the research. N.E.M. performed the thermolysis and sulfation

experiments. J.M., L.S. and N.R. evaluated the molar masses of the plastic feedstocks and thermolysis products. N.E.M. and A.D. conducted materials characterization of plastic waste-based detergents. R.Q. and R.J. performed the computational fluid dynamics studies. G.L. and N.E.M. wrote the original manuscript. All authors contributed to manuscript proofreading and editing.

Competing interests

G.L. and N.E.M. have filed a patent based on this work: PCT/US2024/026720. The remaining authors declare no competing interests.

Additional information

Supplementary information The online version contains supplementary material available at https://doi.org/10.1038/s41893-024-01464-x.

Correspondence and requests for materials should be addressed to Rui Qiao or Guoliang Liu.

Peer review information *Nature Sustainability* thanks Yue Liu, Fan Zhang and the other, anonymous, reviewer(s) for their contribution to the peer review of this work.